crystals

MDPI

Article

Potassium Disorder in the Defect Pyrochlore $KSbTeO_6$: A Neutron Diffraction Study

José Antonio Alonso [1,*], Sergio Mayer [2], Horacio Falcón [2], Xabier Turrillas [3,4] and María Teresa Fernández-Díaz [5]

1 Instituto de Ciencia de Materiales de Madrid Consejo Superior de Investigaciones Científicas., Cantoblanco, E-28049 Madrid, Spain
2 Nanotech (Centro de Investigación en Nanociencia y Nanotecnología), Universidad Tecnológica Nacional-Facultad Regional Córdoba, 5016 Córdoba, Argentina; sergiomayer91@gmail.com (S.M.); hfalcon@frc.utn.edu.ar (H.F.)
3 Institut de Ciència de Materials de Barcelona, Consejo Superior de Investigaciones Científicas, Bellaterra, E-08193 Barcelona, Spain; turrillas@gmail.com
4 ALBA Synchrotron, Cerdanyola del Vallès, E-08290 Barcelona, Spain
5 Institut Laue Langevin, BP 156X, F-38042 Grenoble, France; ferndiaz@ill.eu
* Correspondence: ja.alonso@icmm.csic.es; Tel: +34-91-334-9071; Fax: +34-91-372-0623

Academic Editors: Helmut Cölfen and Silvina Pagola
Received: 25 November 2016; Accepted: 26 December 2016; Published: 13 January 2017

Abstract: $KSbTeO_6$ defect pyrochlore has been prepared from $K_2C_2O_4$, Sb_2O_3, and 15% excess TeO_2 by solid-state reaction at 850 °C. Direct methods implemented in the software EXPO2013 allowed establishing the basic structural framework. This was followed by a combined Rietveld refinement from X-ray powder diffraction (XRD) and neutron powder diffraction (NPD) data, which unveiled additional structural features. $KSbTeO_6$ is cubic, a = 10.1226(7) Å, space group $Fd\bar{3}m$, Z = 8 and it is made of a mainly covalent framework of corner-sharing (Sb,Te)O_6 octahedra, with weakly bonded K^+ ions located within large cages. The large K-O distances, 3.05(3)–3.07(3) Å, and quite large anisotropic atomic displacement parameters account for the easiness of K^+ exchange for other cations of technological importance.

Keywords: pyrochlores; AB_2O_6; $ASbTeO_6$; neutron powder diffraction; ionic diffusion

1. Introduction

Recently, the defect pyrochlore oxide $(H_3O)SbTeO_6$ has been described as an excellent proton conductor [1,2], showing a conductivity (σ) of 10^{-1} S·cm^{-1} at 30 °C under saturated water vapor partial pressure, matching the performance of Nafion© as proton conductor for low-temperature fuel cells. Among the most promising candidates to replace Nafion, the so-called antimonic acids (of general stoichiometry $HSbO_3{\cdot}nH_2O$ or $Sb_2O_5{\cdot}nH_2O$) show a relatively high proton conductivity of ~10^{-4} S·cm^{-1} at room temperature (RT) [3], and some yttrium-doped derivatives reach conductivities as high as 10^{-3} S·cm^{-1} [4]. An even larger σ value of 10^{-1} S·cm^{-1} at 30 °C under saturated water vapor partial pressure was described by Turrillas et al. [5], for an original derivative of the antimonic acid obtained by partial replacement of Sb by Te, giving rise to a well-defined oxide with pyrochlore structure and composition $(H_3O)SbTeO_6$ [5]. The pyrochlore structure is very appealing while searching for materials of high ionic conductivity, since its open framework containing three-dimensional interconnected channels enables H_3O^+ ion diffusion. The general crystallographic formula of pyrochlore oxides is $A_2B_2O_6O'$, consisting of a covalent B_2O_6 network of BO_6 corner-sharing octahedra with an approximate B-O-B angle of 130°, and the A_2O' sub-lattice forming an interpenetrating network which does not interact with the former. It is well known that

both A cations and O′ oxygens may be partially absent in defect pyrochlores with $A_2B_2O_6$ or even AB_2O_6 stoichiometry [6].

The full characterization of the crystal structure of $(H_3O)SbTeO_6$ was performed by neutron diffraction, leading to the location of the protons in the framework [1]. $(H_3O)SbTeO_6$ has been prepared by ion exchange from $KSbTeO_6$ pyrochlore in sulfuric acid at 453 K for 12 h [1,2]. The crystal structure of $KSbTeO_6$ has not been described in detail, although a pioneering study reports the synthesis of the $A(SbTe)O_6$ pyrochlore family (A = K, Rb, Cs, Tl) [7]. The crystal structures of these oxides were defined in the $Fd\bar{3}m$ space group (No. 227), with $Z = 8$. For A = K, the unit–cell parameter reported is a = 10.1133(2) Å. Sb and Te atoms were defined to be statistically distributed at 16*d* Wyckoff sites; oxygen atoms were placed at 48*f* sites, and A cations at 32*e* (*x*,*x*,*x*) Wyckoff positions with x = 0.109, from XRD data [7]. In the present work, we report the ab-initio crystal structure determination of $KSbTeO_6$ from NPD data, followed by a Rietveld refinement from combined XRD and NPD data, yielding complementary information on the K^+ positions.

2. Experimental

$KSbTeO_6$ was prepared by the solid-state reaction between potassium oxalate ($K_2C_2O_4$), TeO_2, and Sb_2O_3 in a 1:2.3:1 molar ratio, providing an excess of TeO_2 to compensate for volatilization losses. The starting mixture was thoroughly ground and heated at 823, 973, 1073, and 1123 K for 24 h at each temperature, with intermediate grindings in order to ensure total reaction.

The initial product characterization was carried out by XRD with a Bruker-AXS D8 Advance diffractometer (40 kV, 30 mA) (Germany) controlled by the DIFFRACT^{PLUS} software, in Bragg–Brentano reflection geometry, with Cu K_α radiation (λ = 1.5418 Å). A nickel filter was used to remove Cu K_β radiation. NPD experiments were carried out in the D2B high-resolution powder diffractometer (λ = 1.595 Å) at the Institut Laue-Langevin, in Grenoble, France. About 2 g of sample was contained in a vanadium can. The full diffraction pattern was collected in 3 h.

The crystal structure was solved ab-initio from NPD data using direct methods and the software EXPO2013 [8]. The model obtained was refined by the Rietveld method [9] with the program FULLPROF (Grenoble, France, version Nov. 2016) [10], from combined XRD and NPD data. A pseudo-Voigt function was chosen to generate the line shape of the diffraction peaks. The following parameters were refined in the final Rietveld fit: scale factor, background coefficients, zero-point error, pseudo-Voigt profile function parameters corrected for asymmetry, atomic coordinates, anisotropic atomic displacement parameters for all atoms, and the occupancy factor of the K^+ positions. The coherent scattering lengths of K, Sb, Te and O were 3.67, 5.57, 5.80 and 5.803 fm, respectively.

3. Results and Discussion

$KSbTeO_6$ oxide was obtained as a well-crystallized powder. The XRD pattern, shown in Figure 1, is characteristic of a pyrochlore-type structure, with a = 10.1226(7) Å. As input data for EXPO2013 [8], the unit–cell parameters, $Fd\bar{3}m$ space group symmetry and unit–cell contents were given: 8 K, 48 O and 16 Sb, due to the similar Sb and Te scattering lengths. NPD data were used for the crystal structure determination, given their monochromaticity, well-defined peak shape, and the large 2θ range covered (from 0 to 159°). EXPO2013 readily gave a structural model with O positions (⅛,⅛,0.429) corresponding to 48*f* Wyckoff sites, Sb positions (½,½,½) corresponding to 16*d* sites, and two possible Wyckoff sites for K: (⅛,⅛,⅛), i.e., 8*a* sites; and (*x*,*x*,*x*), i.e., 32*e* sites with x = 0.248, defined in the origin choice 2 of the space group $Fd\bar{3}m$ (No 227). A combined XRD and NPD Rietveld refinement was carried out in that setting. The Sb and Te atoms were considered to be statistically distributed at (½,½,½) 16*d* Wyckoff sites, and K at (*x*,*x*,*x*) 32*e* sites. The K^+ ions were allowed to shift along the (*x*,*x*,*x*) 32*e* position adopting intermediate x values between those suggested by the ab-initio crystal structure determination. At the stage of refining isotropic atomic displacement parameters, x = 0.1429(6) was reached for the (*x*,*x*,*x*) 32*e* Wyckoff position after convergence, accompanied by large temperature factors (B) of 1.2(2) Å^2.

A further fit improvement was achieved by refining anisotropic atomic displacement parameters, leading to the crystallographic data and Rietveld agreement factors gathered in Table 1.

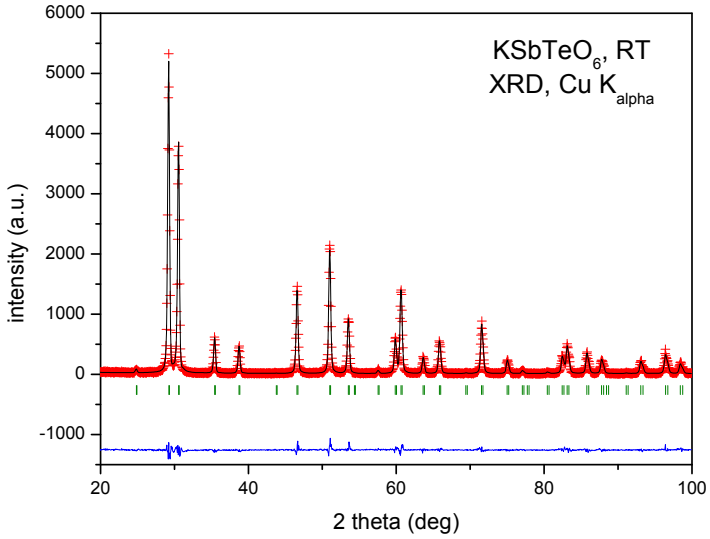

Figure 1. Rietveld-refined XRD pattern of $KSbTeO_6$ at 298 K, characteristic of a cubic pyrochlore phase. The experimental XRD data is represented with red crosses, the calculated profile is shown with a black solid line, and their difference is shown at the bottom (blue line). Vertical green symbols indicate allowed peak positions.

Table 1. Unit–cell, fractional atomic coordinates, atomic displacement parameters, refined occupancy factors and Rietveld agreement factors of $KSbTeO_6$ in the cubic space group $Fd\bar{3}m$ (No. 227), with Z = 8.

Crystal Data						
Cubic, $Fd\bar{3}m$				X-ray radiation, λ = 1.5418 Å		
				Neutron radiation, λ = 1.595 Å		
a = 10.1226(7) Å V = 1037.22(12) Å^3				Particle morphology: powder Z = 8		
Rietveld Agreement Factors						
XRD data R_p = 7.55% R_{wp} = 11.77% R_{exp} = 9.11% R_{Bragg} = 3.40% χ^2 = 1.67				NPD data R_p: 4.75% R_{wp}: 6.27% R_{exp}: 3.85% R_{Bragg} = 3.59% χ^2 = 2.65		
1801 data points				3240 data points		
Atomic Coordinates, Isotropic Atomic Displacement Parameters (Å^2) and Refined Occupancy Factors						
	x	*y*	*z*	U_{eq}	Occupancy	
K	0.126(3)	0.126(3)	0.126(3)	0.060(4)	0.256(4)	
Sb1	0.50000	0.50000	0.50000	0.0037(3)		
Te1	0.50000	0.50000	0.50000	0.0037(3)		
O1	0.42760(9)	0.12500	0.12500	0.0099(3)		
Anisotropic Atomic Displacement Parameters (Å^2)						
	U^{11}	U^{22}	U^{33}	U^{12}	U^{13}	U^{23}
K	0.055(3)	0.055(3)	0.055(3)	0.025(8)	0.025(8)	0.025(8)
Sb	0.0037(3)	0.0037(3)	0.0037(3)	−0.0004(3)	−0.0004(3)	−0.0004(3)
Te	0.0037(3)	0.0037(3)	0.0037(3)	−0.0004(3)	−0.0004(3)	−0.0004(3)
O	0.0075(4)	0.0111(3)	0.0111(3)	0.0	0.0	−0.0065(4)

In the final Rietveld refinement, the x parameter in the 32*e* position shifted to 0.126(3). Thus, K practically occupies the (⅛,⅛,⅛) 8*a* Wyckoff sites. The main interatomic distances and angles are shown in Table 2. Figures 1 and 2 illustrate the good agreement between the observed and calculated XRD and NPD patterns, respectively.

The Sb:Te ratio could not be refined, given the similar scattering factors (or scattering lengths for neutrons) of both elements using XRD or NPD. This ratio has to be 1:1 if K fully resides at 8*a* Wyckoff sites, or at 32*e* sites with an occupation of 1/4. The excess of TeO_2 added to compensate for volatilization losses could also result in a slight over-occupation of the position with Te; therefore, an even lower occupation of the K position would occur. To address this problem, the occupancy of K was also refined: it converged to 1 atom per formula unit, within standard deviations (see Table 1), thus confirming the 1:1 Sb:Te ratio.

Table 2. Selected interatomic distances and angles for $KSbTeO_6$ at 298 K.

Distances (Å)	
K-O (x3)	3.05(3)
K-O′ (x3)	3.07(3)
(Sb,Te)-O (x6)	1.9338(6)
Angles (°)	
O-(Sb,Te)-O	86.10(3)
	93.90(3)
(Sb,Te)-O-(Sb,Te)	135.45(2)

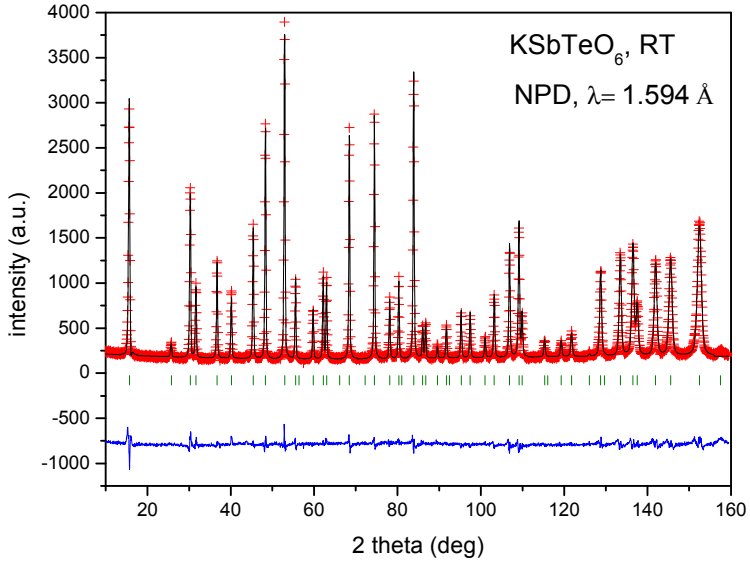

Figure 2. Rietveld-refined NPD pattern of $KSbTeO_6$ at 298 K in the cubic$Fd\bar{3}m$ space group. The experimental NPD data is represented with red crosses, the calculated profile is shown with a black solid line, and their difference is shown at the bottom (blue line). Vertical green symbols indicate allowed peak positions.

Figure 3 displays the pyrochlore structure of $KSbTeO_6$, which can be described as composed of a mainly covalent network of $(Sb,Te)O_6$ units sharing corners, with a (Sb,Te)-O-(Sb,Te) angle of 135.45(2)° (Table 2). The cage-like holes within this network contain the K^+ ions statistically distributed at 32*e* Wyckoff positions, with four times the required multiplicity to host K^+ ions (eight per unit cell); thus, only one in four lobes within each K^+ cluster shown in Figure 3 must be considered as occupied.

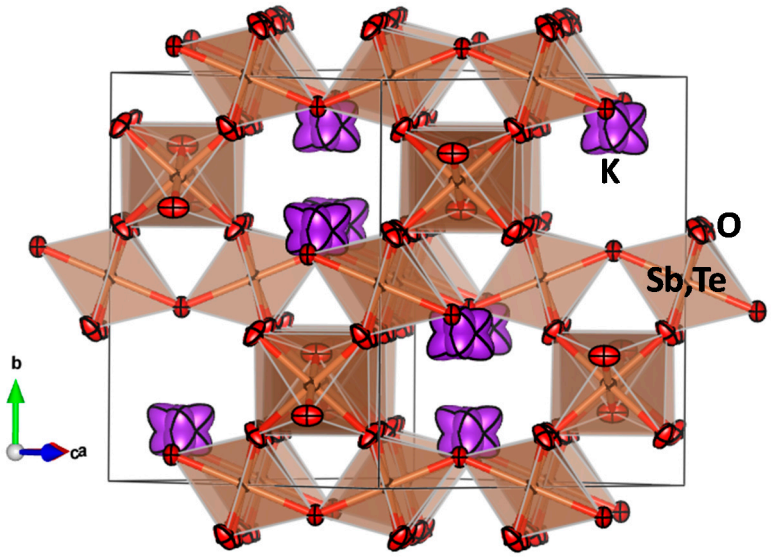

Figure 3. View of the $KSbTeO_6$ pyrochlore structure approximately along the [$1\bar{1}0$] direction. It consists of a mainly covalent framework of (Sb,Te)O_6 octahedra sharing vertices, forming large cages wherein K^+ ions are distributed at 32*e* Wyckoff sites with 1/4 occupancy and large anisotropic atomic displacement parameters.

The so-called (Sb,Te)O_6 octahedra are in fact slightly axially distorted, but they contain six equal (Sb,Te)-O interatomic distances of 1.9338(6) Å (Table 2), which compare well with 1.96 Å, Shannon's ionic radius sum [11].

The location of K^+ ions at 32*e* Wyckoff sites has been previously reported for the $ASbTeO_6$ series [6]. It is noteworthy that, in pioneering work on defect AB_2O_6 pyrochlores [12–14], the position of the A atoms was thought to be 8*a*; later on, the occupancy of (*x*,*x*,*x*) 32*e* positions, with *x* close to 1/8 was suggested [15–17]. For $KSbTeO_6$, the present work underlines the different results obtained refining isotropic atomic displacement parameters [*x*(K) = 0.1429(6)], thus with K^+ at 32*e* Wyckoff sites; or anisotropic atomic displacement parameters, resulting in *x*(K) = 0.126(3), very close to 1/8 and thus equivalent (within experimental error) to 8*a* Wyckoff sites. If the K^+ positions are fixed at the 8*a* site, the Rietveld fit does not improve and the atomic displacement parameters of all atoms remain similar.

The K^+ coordination is shown in Figure 4, with K-O distances of 3.05 and 3.07 Å (Table 2) in a pseudo-octahedral coordination to oxygen atoms. In defect AB_2O_6 pyrochlores, it is worth recalling that for *x* equal or close to zero, the A atom can be considered as coordinated to six oxygen atoms only, forming a corrugated hexagon normal to the three-fold axis along the [111] direction. For increasing *x*, some new A-O distances decrease in such a way that for *x* equal to 1/8 (8*a* Wyckoff position in the $Fd\bar{3}m$ space group), A atoms occupy the center of a wide cage formed by 18 oxygens, six of them at relatively short distances (3O + 3O′), and 12 at larger distances (3O″ + nine-additional oxygens, which are not shown in Figure 4).

In the present structural description, with *x* virtually 1/8, quite large anisotropic thermal ellipsoids (Figure 4) were determined, with r.m.s. displacements of 0.324 Å and 0.172 Å along the long and short ellipsoid axes, respectively. Furthermore, the crystal structure described accounts for the large mobility of K^+ ions within the pyrochlore cages and the easiness of ion exchange that leads to $(H_3O)SbTeO_6$ by treatment in H_2SO_4 [1,2], thus enabling the conversion of the present material in a technologically important compound with exceedingly high ionic conductivity.

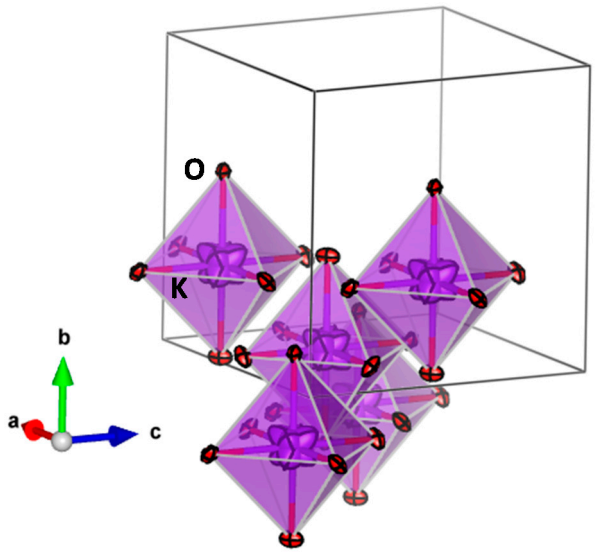

Figure 4. Close up of the coordination polyhedra around K^+ ions enhancing the lobes of the anisotropic thermal ellipsoids, with K^+ statistically occupying one in four lobes within each polyhedron. (Sb,Te)O_6 octahedra are not represented for clarity.

4. Conclusions

$KSbTeO_6$ exhibits a defect pyrochlore structure defined in the cubic $Fd\bar{3}m$ symmetry. The mainly covalent network formed by vertex-sharing (Sb,Te)O_6 octahedra enables weak interatomic interactions with K^+ ions. A combined XRD and NPD study showed that K^+ occupies 32*e* Wyckoff sites indistinguishable (within experimental error) from 8*a* sites, placed in the center of a large cage determined by 6 K-O distances in the range 3.05(3)–3.07(3) Å. The quite big anisotropic atomic displacement parameters account for the easiness of ion exchange of this material to yield a product of technological importance, $(H_3O)SbTeO_6$ [2].

Acknowledgments: We thank the financial support of the Spanish MINECO to the project MAT2013-41099-R. We are grateful to the Institut Laue-Langevin (ILL) in Grenoble for making all the facilities available.

Author Contributions: José Antonio Alonso and Xabier Turrillas conceived and designed the experiments; Sergio Mayer, Horacio Falcón and María Teresa Fernández-Díaz performed the experiments; José Antonio Alonso and Xabier Turrillas analyzed the data; they all wrote the paper.

Conflicts of Interest: The authors declare no conflict of interest.

References

1. Alonso, J.A.; Turrillas, X. Location of H^+ sites in the fast proton-conductor $(H_3O)SbTeO_6$ pyrochlore. *Dalton Trans.* **2005**, 865–867. [CrossRef] [PubMed]
2. Soler, J.; Lemus, J.; Pina, M.P.; Sanz, J.; Aguadero, A.; Alonso, J.A. Evaluation of the pyrochlore $(H_3O)SbTeO_6$ as a candidate for electrolytic membranes in PEM fuel cells. *J. New Mater. Electrochem. Syst.* **2009**, *12*, 77–80.
3. England, W.A.; Cross, M.G.; Hamnett, A.; Wiseman, P.J.; Goodenough, J.B. Fast proton conduction in inorganic ion-exchange compounds. *Solid State Ion.* **1980**, *1*, 231–249. [CrossRef]
4. Ozawa, K.; Wang, J.; Ye, J.; Sakka, Y.; Amano, M. Preparation and Some Electrical Properties of Yttrium-Doped Antimonic Acids. *Chem Mater.* **2003**, *15*, 928–934. [CrossRef]
5. Turrillas, X.; Delabouglise, G.; Joubert, J.G.; Fournier, T.; Muller, J. Un nouveau conducteur protonique $HSbTeO_6 \cdot xH_2O$. Conductivite en fonction de la temperature et de la pression partielle de vapeur d'eau. *Solid State Ion.* **1985**, *17*, 169–174.
6. Subramanian, M.; Aravamudan, G.; Subba Rao, G.V. Oxide pyrochlores—A review. *Prog. Solid State Chem.* **1983**, *15*, 55–143. [CrossRef]

7. Alonso, J.A.; Castro, A.; Rasines, I. Study of the defect pyrochlores A(SbTe)O_6 (A = K, Rb, Cs, Tl). *J. Mater. Sci.* **1988**, *23*, 4103–4107. [CrossRef]
8. Altomare, A.; Cuocci, C.; Giacovazzo, C.; Moliterni, A.; Rizzi, R.; Corriero, N.; Falcicchio, A. EXPO2013: A kit of tools for phasing crystal structures from powder data. *J. Appl. Cryst.* **2013**, *46*, 1231–1235. [CrossRef]
9. Rietveld, H.M. A profile refinement method for nuclear and magnetic structures. *J. Appl. Crystallogr.* **1969**, *2*, 65–71. [CrossRef]
10. Rodríguez-Carvajal, J. Recent advances in magnetic structure determination by neutron powder diffraction. *Physica B* **1993**, *192*, 55–69. [CrossRef]
11. Shannon, R.D. Revised effective ionic radii and systematic studies of interatomic distances in halides and chalcogenides. *Acta Crystallogr.* **1976**, *A32*, 751–767. [CrossRef]
12. Babel, D.; Pausegang, G.; Werner, V. Die Struktur einiger Fluoride, Oxide und Oxidfluoride AMe_2X_6: Der $RbNiCrF_6$-Typ. *Zeitschrift für Naturforschung B* **1967**, *22*, 1219–1220. [CrossRef]
13. Darriet, B.; Rat, M.; Galy, J.; Hagenmuller, R. Sur quelques nouveaux pyrochlores des systemes $MTO_3 - WO_3$ et $MTO_3 - TeO_3$ (M = K, Rb, Cs, Tl; T = Nb, Ta). *Mater. Res. Bull.* **1971**, *6*, 1305–1315. [CrossRef]
14. El Haimouti, A.; Zambon, D.; El-Ghozzi, M.; Avignant, D.; Leroux, F.; Daoud, M.; El Aatmani, M. Synthesis, structural and physico-chemical characterization of new defect pyrochlore-type antimonates $K_{0.42}Ln_{y'}Sb_2O_{6+z'}$ and $Na_{0.36}Ln_ySb_2O_{6+z}$ ($0 < y, y'; ' z, z' < 1$; Ln = Y, Eu and Gd) prepared by soft chemistry route. *J. Alloy. Compd.* **2004**, *363*, 130–137. [CrossRef]
15. Fourquet, J.L.; Javobini, C.; de Pape, R. Les pyrochlores AIB_2X_6: Mise en evidence de l'occupation par le cation AI de nouvelles positions cristallographiques dans le groupe d'espace $Fd\bar{3}m$. *Mater. Res. Bull.* **1973**, *8*, 393–403. [CrossRef]
16. Pannetier, J. Energie electrostatique des reseaux pyrochlore. *J. Phys. Chem. Solids* **1973**, *34*, 583–589. [CrossRef]
17. Castro, A.; Rasines, I.; Sanchez-Martos, M.C. Novel deficient pyrochlores A(MoSb)O_6 (A = Rb, Cs). *J. Mater. Sci. Lett.* **1987**, *6*, 1001–1003. [CrossRef]